Energy level alignment at metal/organic semiconductor interfaces: "Pillow" effect, induced density of interface states, and charge neutrality level

H. Vázquez, Y. J. Dappe, J. Ortega, and F. Flores
Departamento de Física Teórica de la Materia Condensada, Universidad Autónoma de Madrid, E-28049 Madrid, Spain

(Received 1 December 2006; accepted 13 February 2007; published online 10 April 2007)

A unified model, embodying the "pillow" effect and the induced density of interface states (IDIS) model, is presented for describing the level alignment at a metal/organic interface. The pillow effect, which originates from the orthogonalization of the metal and organic wave functions, is calculated using a many-body linear combination of atomic orbitals Hamiltonian, whereby electron long-range interactions are obtained using an expansion in the metal/organic wave function overlap, while the electronic charge of both materials remains unchanged. This approach yields the pillow dipole and represents the first effect induced by the metal/organic interaction, resulting in a reduction of the metal work function. In a second step, we consider how charge is transferred between the metal and the organic material by means of the IDIS model: Charge transfer is determined by the relative position of the metal work function (corrected by the pillow effect) and the organic charge neutrality level, as well as by an interface parameter S, which measures how this potential difference is screened. In our approach, we show that the combined IDIS-pillow effects can be described in terms of the original IDIS alignment corrected by a screened pillow dipole. For the organic materials considered in this paper, we see that the IDIS dipole already represents most of the realignment induced at the metal/organic interface. We therefore conclude that the pillow effect yields minor corrections to the IDIS model. © *2007 American Institute of Physics*. [DOI: 10.1063/1.2717165]

I. INTRODUCTION

The field of organic electronics has been attracting the attention of the scientific community over the last years. The appearance of new electronic devices based on organic materials such as light-emitting diodes, thin-film transistors, or solar cells,[1] some of which are already on the market, has stimulated research in organic semiconducting materials. In all of these cases, processes taking place at interfaces are especially important; in particular, metal/organic interfaces will be present whenever metallic electrodes are used (as is the case of most devices) to inject charge into or extract charge from the organic layer(s). Since the process of charge injection ultimately determines the performance of these devices, a detailed understanding of the processes taking place at metal/organic interfaces is essential. Central to this issue is the problem of the molecular level alignment at these interfaces: The relative position of the energy levels of the metal and the organic material once the interface is formed determines the injection barrier at the metal/organic interface. Since the Schottky barrier is the single most important parameter limiting charge injection,[2] knowledge of the fundamental mechanisms governing the barrier formation is mandatory. Although inorganic semiconductor interfaces offer inspiration for understanding the interface energy level alignment, the topic at metal/organic interfaces is still not fully understood.

The Schottky-Mott limit, which consists on the simple alignment of the vacuum levels of both materials, was soon disproved,[3,4] and interface dipoles and the (stronger or weaker) pinning of the Fermi level were observed experimentally for different metal/organic interfaces.[5] Several models have been proposed in the literature to explain this behavior: (i) Chemically reactive interfaces[6–10] can be analyzed theoretically with relative ease using density-functional theory (DFT) based methods. These junctions are characterized by the formation of chemisorption-induced gap states and the formation of metal-absorbate bonds. While obviously of great importance, chemisorptive interfaces, however, suffer from lack of generality since the outcome of a particular reaction is unpredictable; the results for one reactive interface are difficult to extrapolate to other cases, so that research in these reactive interfaces advances in a stepwise manner. (ii) The orientation of permanent molecular dipoles obviously affects the molecular level alignment since the component of these dipoles in the direction perpendicular to the interfaces will translate into a potential drop across the interface.[11,12] However, since relatively few molecules exhibit a permanent dipole, this effect will not be operating on many interfaces. (iii) The charge transfer between the metal and the organic material has been analyzed using the organic ionization and affinity levels.[6,7] (iv) The compression of the metal electronic tail due to the presence of adsorbed molecules[13–15] gives rise to a potential drop at the interface. This charge rearrangement, termed "pillow" effect, has the effect of reducing the metal work function and will be discussed below within our formalism.

In spite of these proposed mechanisms, however, a complete, consistent model for the energy level alignment is still

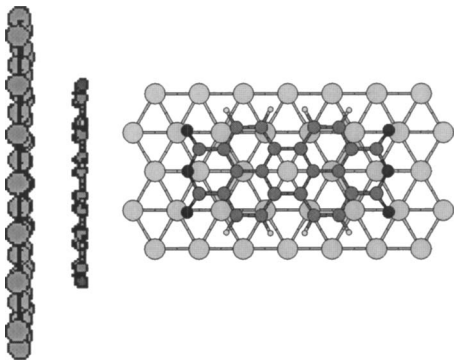

FIG. 1. Side (left) and top (right) views of an organic molecule deposited flat over a metal surface, whose last plane is shown.

lacking. In a series of papers,[16–18] we proposed a model for weakly interacting interfaces based on the concepts of induced density of states (DOS) and charge neutrality level (CNL). This model generalizes some of the mechanisms described previously and its formalism allows for their straightforward incorporation into our description, as will be seen.

While reactive or interdiffusive interfaces are obviously important, our work has focused on the opposite regime: In the limit of weak interaction, we consider abrupt, "ideal" interfaces for which we take Au(111) as a prototype and analyze the energy level alignment. In this paper we consider interfaces between Au and the following organic materials: 3,4,9,10-perylenetetracarboxylic dianhydride (PTCDA), 3,4,9,10-perylenetetracarboxylic bisbenzimidazole (PTCBI), 4,4′,*N*,*N*′-dicarbazolyl biphenyl (CBP), and copper phthalocyanine (CuPc).

We present a combined theoretical description of both the pillow effect and the induced DOS, which up to now had been presented independently. We compare the merits of these two effects, which will be present at any metal/organic interface since they are intrinsic properties of interfaces, and then present a unified theoretical model which incorporates both mechanisms. Our approach follows a method successfully used to calculate the electronic properties of solids and molecules,[19–21] combined with an expansion of the metal/organic interaction in terms of the overlap between both media. This is reminiscent of other chemical methods (e.g., symmetric perturbation methods[22–26] or symmetry-adapted perturbation theory[27–29]) and is closely related to the constrained space orbital variation (CSOV) method of Bagus *et al.*,[30] where orthogonalization effects are first considered and charge transfer is then taken into account.

II. MODEL

Figure 1 schematically presents the structure of the systems we discuss in the present paper: Experimental evidence[10,31–34] indicates that many organic molecules are deposited flat on the metal surface. Since intermolecular interactions are weak and do not induce a DOS in the molecular gap (the key quantity governing the level alignment, as will be seen), we can restrict our analysis to a single molecule deposited flat on the Au surface, as depicted schematically in Fig. 1.

It is convenient to start our discussion by introducing an approximation to the linear combination of atomic orbitals Hamiltonian[19] for Au ($\hat{H}_1$) and the organic molecule ($\hat{H}_2$).

$$\hat{H}_1 = \sum_{\nu\sigma} (\varepsilon_\nu + V_{\nu\nu}^{\mathrm{psp}})\hat{n}_{\nu\sigma} + \sum_{\nu\mu,\sigma} \hat{T}_{\nu\mu}\hat{c}_{\nu\sigma}^{+}\hat{c}_{\mu\sigma} + \sum_{\nu} U_\nu \hat{n}_{\nu\uparrow}\hat{n}_{\nu\downarrow} + \frac{1}{2}\sum_{\nu\mu} [J_{\nu\mu}\hat{n}_{\nu\sigma}\hat{n}_{\mu\bar{\sigma}} + (J_{\nu\mu} - J_{\nu\mu}^{x})\hat{n}_{\nu\sigma}\hat{n}_{\mu\sigma}], \quad (1)$$

with a similar equation for $\hat{H}_2(\nu,\mu \rightarrow \nu',\mu')$,

$$\hat{H}_2 = \sum_{\nu'\sigma} (\varepsilon_{\nu'} + V_{\nu'\nu'}^{\mathrm{psp}})\hat{n}_{\nu'\sigma} + \sum_{\nu'\mu',\sigma} \hat{T}_{\nu'\mu'}\hat{c}_{\nu'\sigma}^{+}\hat{c}_{\mu'\sigma} + \sum_{\nu'} U_{\nu'}\hat{n}_{\nu'\uparrow}\hat{n}_{\nu'\downarrow} + \frac{1}{2}\sum_{\nu'\mu'} [J_{\nu'\mu'}\hat{n}_{\nu'\sigma}\hat{n}_{\mu'\bar{\sigma}} + (J_{\nu'\mu'} - J_{\nu'\mu'}^{x})\hat{n}_{\nu'\sigma}\hat{n}_{\mu'\sigma}], \quad (2)$$

where

$$\hat{T}_{\nu\mu} = t_{\nu\mu} + V_{\nu\mu}^{\mathrm{psp}} + \sum_{\lambda\sigma'} h_{\lambda,\nu\mu}\hat{n}_{\lambda\sigma'} - \sum_{\lambda\sigma'} h_{\lambda,\nu\mu}^{x}\hat{n}_{\lambda\sigma}. \quad (3)$$

In Eqs. (1) and (2), we use a Löwdin orthogonal basis: $\phi_\nu = \Sigma_\mu (S^{-1/2})_{\nu\mu}\psi_\mu$, where ψ_μ are the atomic orbitals (similarly for $\psi_{\mu'}$). In these equations, ε_ν and $T_{\nu\mu}$ are the one-electron diagonal energies and hoppings, while U_ν, $J_{\nu\mu}$, and $J_{\nu\mu}^{x}$ are the on-site, intersite, and intersite exchange Coulomb integrals; $h_{\lambda,\nu\mu}$ and $h_{\lambda,\nu\mu}^{x}$ are three-center integrals which correspond to the modification of the hopping elements ν and μ due to the charge density λ.

Hamiltonians 1 and 2 have been used to successfully calculate the electronic structure of solids[19] and organic molecules;[20,21] Eqs. (1) and (2) are simplifications of the full Hamiltonian used in these references, where other terms (such as nearest-neighbor four-center interactions, for instance) are included. Our interest now is to analyze the electronic properties of the system when the metal ($\hat{H}_1$) and the organic molecule ($\hat{H}_2$) are brought close to each other and are forming an ideal interface. Two main effects appear:

(i) Due to the overlap between the metal and the adsorbed molecule, wave functions are renormalized and an induced pillow dipole appears at the interface. The orthogonalization of the metal and organic wave functions pushes the metal electronic tail "into" the metal, which gives rise to a lowering of the metal work function (i.e., towards less negative values).

(ii) As discussed in Refs. 16–18, the chemical interaction between metal and molecule gives rise to charge transfer between them, which represents an important contribution to the interface dipole.

These two effects are analyzed in more detail below.

III. "PILLOW" EFFECT

The compression of the metal wave function due to the adsorbed molecules can be analyzed within our formalism by considering the long-range interactions $J_{\nu\mu}$ and $h_{\lambda,\nu\mu}$ defined

above and their modification due to the overlap with the organic wave functions (orbitals ϕ_ν and $\phi_{\nu'}$).

Consider first the intersite Coulomb interaction $J_{\lambda\mu}$,

$$J_{\lambda\mu} = \int \phi_\lambda^2(\mathbf{r}) \frac{1}{|\mathbf{r}-\mathbf{r}'|} \phi_\mu^2(\mathbf{r}') \tag{4}$$

(λ is going to be an orbital located far away from the interface; a probe for the electrostatic dipole induced at the interface). When the wave functions ϕ_ν and $\phi_{\nu'}$ overlap ($S_{\nu\nu'} \neq 0$), $J_{\lambda\nu}$ should be recalculated by introducing a new Löwdin wave function $\Phi_\mu(\mathbf{r}')$ given by

$$\Phi_\mu(\mathbf{r}') = \sum_i (S^{-1/2})_{\mu i} \phi_i(\mathbf{r}'), \tag{5}$$

where $i \equiv (\nu, \nu')$, and ϕ_i are the Löwdin wave functions of the uncoupled media. Since $S_{\mu\mu'}$ are small, we expand $S^{-1/2}$ up to second order in S and write

$$\Phi_\mu = \phi_\mu - \frac{1}{2}\sum_{\mu'} S_{\mu\mu'}\phi_{\mu'} + \frac{3}{8}\sum_{\mu'\nu} S_{\mu\mu'}S_{\mu'\nu}\phi_\nu. \tag{6}$$

By replacing Eq. (6) in Eq. (4) we find the following change in $J_{\lambda\mu}$:

$$\begin{aligned}\delta J_{\lambda\mu} = &-\sum_{\mu'} S_{\mu\mu'} \int \phi_\lambda^2 \frac{1}{|\mathbf{r}-\mathbf{r}'|}\phi_\mu\phi_{\mu'} \\ &+ \frac{1}{4}\sum_{\mu'} S_{\mu\mu'}^2 \int \phi_\lambda^2 \frac{1}{|\mathbf{r}-\mathbf{r}'|}\phi_{\mu'}^2 \\ &+ \frac{3}{4}\sum_{\mu'} S_{\mu\mu'}^2 \int \phi_\lambda^2 \frac{1}{|\mathbf{r}-\mathbf{r}'|}\phi_\mu^2 \\ &+ \frac{1}{4}\sum_{\mu'\mu''} S_{\mu\mu'}S_{\mu\mu''} \int \phi_\lambda^2 \frac{1}{|\mathbf{r}-\mathbf{r}'|}\phi_{\mu'}\phi_{\mu''} \\ &+ \frac{3}{4}\sum_{\mu',\nu\neq\mu} S_{\mu\mu'}S_{\mu'\nu} \int \phi_\lambda^2 \frac{1}{|\mathbf{r}-\mathbf{r}'|}\phi_\mu\phi_\nu. \end{aligned} \tag{7}$$

Since we are assuming orbital λ to be far from the surface, we can approximate the electronic density λ by a point charge, so that the potential created by charge densities μ and μ' is calculated at the center of λ, eliminating the integration in $\mathbf{r}$. We then expand $|\mathbf{r}-\mathbf{r}'|$ around $|\mathbf{r}-\mathbf{r}_0|$ (where $\mathbf{r}_0$ is the midpoint between orbitals μ and μ', see Fig. 2), and write

$$\frac{1}{|\mathbf{r}-\mathbf{r}'|} \simeq \frac{1}{|\mathbf{r}-\mathbf{r}_0|} + \nabla\left[\frac{1}{|\mathbf{r}-\mathbf{r}'|}\right]\Delta\mathbf{r}' + \cdots, \tag{8}$$

with $\Delta\mathbf{r}' = \mathbf{r}' - \mathbf{r}_0$. Using this in Eq. (7), and taking into account that the potential created by the charge $n_{\mu\sigma}$ on λ is given by $J_{\lambda\mu}n_{\mu\sigma}$, we conclude that the overlaps between orbitals μ and μ' give rise to the following dipole $D_{\mu\sigma}$ at the interface:

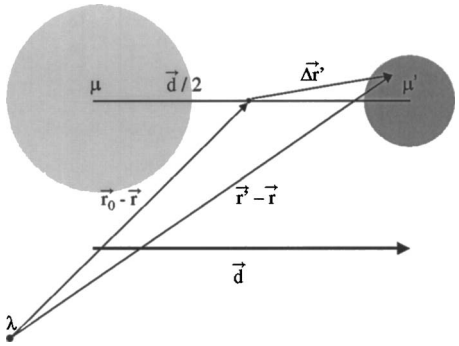

FIG. 2. Au (left) and organic (right) orbitals separated by a distance **d**. To simplify the integrals of our calculations, we approximate the probe electronic density λ by a point charge, eliminating the integration over **r**, and we expand (since λ is located far from the surface) the distance $|\mathbf{r}-\mathbf{r}'|$, placing the origin of integration in $\mathbf{r}'$ at the midpoint between orbitals μ and μ', as discussed in the text.

$$\begin{aligned} D_{\mu\sigma} = n_{\mu\sigma}\Bigg[&-\sum_{\mu'} S_{\mu\mu'} \int \Delta\mathbf{r}'\,\phi_{\mu'}\phi_\mu \\ &+ \frac{1}{4}\sum_{\mu'} S_{\mu\mu'}^2 \int \Delta\mathbf{r}'\,\phi_{\mu'}^2 + \frac{3}{4}\sum_{\mu'} S_{\mu\mu'}^2 \int \Delta\mathbf{r}'\,\phi_\mu^2 \\ &+ \frac{1}{4}\sum_{\mu'\mu''} S_{\mu\mu'}S_{\mu\mu''} \int \Delta\mathbf{r}'\,\phi_{\mu''}\phi_{\mu'} \\ &+ \frac{3}{4}\sum_{\mu',\nu\neq\mu} S_{\mu\mu'}S_{\mu'\nu} \int \Delta\mathbf{r}'\,\phi_\mu\phi_\nu \Bigg], \end{aligned} \tag{9}$$

with a similar expression for $D_{\mu'\sigma}$ (with primed and unprimed indices replaced).

A similar argument can be used to analyze how $h_{\lambda,\nu\mu}$ contributes to the pillow effect: Using Eq. (6) for ϕ_μ and ϕ_ν allows us to calculate $\delta h_{\lambda,\nu\mu}$ and to obtain the following dipole $D_{\nu\mu\sigma}$:

$$\begin{aligned} D_{\nu\mu\sigma} = n_{\nu\mu\sigma}\Bigg[&-\frac{1}{2}\sum_{\nu'} S_{\nu\nu'} \int \Delta\mathbf{r}'\,\phi_{\nu'}'\phi_\mu \\ &- \frac{1}{2}\sum_{\mu'} S_{\mu\mu'} \int \Delta\mathbf{r}'\,\phi_{\mu'}\phi_\nu \\ &+ \frac{1}{4}\sum_{\mu'} S_{\mu\mu'}S_{\mu'\nu} \int \Delta\mathbf{r}'\,\phi_{\mu'}^2 \\ &+ \frac{3}{8}\sum_{\nu'} S_{\nu\nu'}S_{\nu'\mu} \int \Delta\mathbf{r}'\,\phi_\mu^2 \\ &+ \frac{3}{8}\sum_{\mu'} S_{\mu\mu'}S_{\mu'\nu} \int \Delta\mathbf{r}'\,\phi_\nu^2 \Bigg], \end{aligned} \tag{10}$$

with similar equations for $D_{\mu\nu\sigma}$ (ν and μ interchanged), $D_{\nu'\mu'\sigma}$, and $D_{\mu'\nu'\sigma}$ (primed quantities replacing unprimed ones).

Equations (9) and (10) define the dipoles induced by the pillow effect. Notice that for this calculation, n_μ and $n_{\mu'}$ are assumed to be the same as for the noninteracting case, a reasonable assumption since the weak interaction between

both systems is not likely to induce significant changes in the electron density within each material, and implies not including charge transfer at this stage (this will be done within the IDIS model, see below). Notice too that the pillow effect appears only with the overlap between the wave functions of both materials.

Although Eqs. (9) and (10) define the complete electrostatic dipole we are looking for, in our calculations we have used a simplified version of these. First, we neglect the integrals $\int \Delta\mathbf{r}' \phi_\nu \phi_\mu$ or $\int \Delta\mathbf{r}' \phi_{\nu'} \phi_{\mu'}$; the reason is that the pairs ϕ_ν and ϕ_μ (or $\phi_{\nu'}$ and $\phi_{\mu'}$) are already orthogonal for the noninteracting case, since they both belong to the same subsystem (the metal or the organic molecule), and we can therefore expect these integrals to be small. Second, in our calculations, we have not considered the term $D_{\nu\mu\sigma}$ as it is proportional to $n_{\nu\mu\sigma}$, which is assumed to be small.

With these approximations, we have

$$D_{\mu\sigma} \simeq n_{\mu\sigma}\left[-\sum_{\mu'} S_{\mu\mu'} \int \Delta\mathbf{r}' \phi_{\mu'} \phi_\mu + \frac{1}{4}\sum_{\mu'} S^2_{\mu\mu'} \int \Delta\mathbf{r}' \phi^2_{\mu'} + \frac{3}{4}\sum_{\mu'} S^2_{\mu\mu'} \int \Delta\mathbf{r}' \phi^2_{\mu} \right]. \tag{11}$$

From Eq. (11), if we consider orbitals $\mu\sigma$ (metal) and $\mu'\sigma$ (organic molecule), we can associate the following dipole with that "bond:"

$$D^{\text{pillow}}_{\mu\mu'\sigma} = -(n_{\mu\sigma} + n_{\mu'\sigma}) S_{\mu\mu'} \int \Delta\mathbf{r}' \phi_{\mu'} \phi_\mu + \left(\frac{n_{\mu\sigma}}{4} + \frac{3n_{\mu'\sigma}}{4}\right) S^2_{\mu\mu'} \int \Delta\mathbf{r}' \phi^2_{\mu'} + \left(\frac{n_{\mu'\sigma}}{4} + \frac{3n_{\mu\sigma}}{4}\right) S^2_{\mu\mu'} \int \Delta\mathbf{r}' \phi^2_{\mu}. \tag{12}$$

If we now take $\mathbf{r}_0$ as the midpoint between atoms μ and μ', it is easy to see (see Fig. 2) that $\int \Delta\mathbf{r}' \phi^2_{\mu'} = \mathbf{d}/2$ and $\int \Delta\mathbf{r}' \phi^2_{\mu} = -\mathbf{d}/2$ (assuming ϕ^2_μ and $\phi^2_{\mu'}$ to have inversion symmetry). This reduces the pillow dipole to

$$D^{\text{pillow}}_{\mu\mu'\sigma} = -(n_{\mu\sigma} + n_{\mu'\sigma}) S_{\mu\mu'} \int \Delta\mathbf{r}' \phi_{\mu'} \phi_\mu + (n_{\mu\sigma} - n_{\mu'\sigma}) S_{\mu\mu'} \frac{\mathbf{d}}{4}. \tag{13}$$

In our calculations we have used Eq. (13) to obtain the induced dipole resulting from the overlap between the metal and molecular atoms, which is associated with the pillow effect. The dipole points from the metal to the organic molecule, corresponding to electrons being transferred in the opposite direction. This dipole translates into a potential drop at the interface, characterized by an interface dipole Δ, according to

$$\Delta = 4\pi D/A, \tag{14}$$

where D is the corresponding dipole [Eq. (13) summed over all $\mu - \mu'$ pairs] and A is the area associated with each molecule.

IV. INDUCED DENSITY OF INTERFACE STATES DIPOLE

Since this model has been described previously in the context of metal/organic interfaces,[16–18] here we will merely summarize the main physical ideas.

Within the IDIS model, the central quantity is the CNL. The interaction between the metal and the organic material gives rise to a shift and broadening of the molecular levels. For an energy-independent interaction [taking $G_{6s}(E_F)$ and $\Sigma(E_F)$,[16] a good approximation near the gap], the broadening of each state has a Lorentzian shape. Thus, due to the chemical interaction with the metal, the initial discrete distribution of molecular states is broadened into a continuum DOS; in particular, the former energy gap of the organic material is now "filled" with induced DOS, which is precisely the IDIS. The CNL position is such that the integrated induced DOS up to the CNL yields the number of electrons of the isolated molecule,

$$N = \int_{-\infty}^{\text{CNL}} \rho_{\text{IDIS}} dE. \tag{15}$$

The CNL tends to align with the metal work function (in the case of metal/organic interfaces) or with the CNL of the other material (at organic heterojunctions): If the organic CNL is higher (i.e., closer to the vacuum) than the metal work function (for the case of metal/organic interfaces), electrons will be transferred from the organic material to the metal. This gives rise to an electrostatic dipole at the interface, which shifts the relative position of both materials, in the direction of aligning the CNL and ϕ_M. The stronger or weaker degree of alignment is determined by the screening at the interface, as will be discussed below.

Thus, the induced DOS plays a major role in the alignment since it acts as a buffer for charge exchange and thus pins the interface Fermi level more strongly or weakly near the CNL.

The CNL represents a kind of electronegativity or effective Fermi level of the organic material at the interface. On perspective, it can be thought of an extension of the original ideas of Mülliken and Pauling of determining atomic electronegativities using the average $(I+A)/2$ of the ionization (I) and affinity (A) levels of atoms, where the value $(I+A)/2$ was used to predict the direction of charge transfer between atoms. The concept of CNL was formally developed in the context of inorganic semiconductors as the average of the optical gap over the Brillouin zone;[35] again, the relative value of the CNL with the metal work function (at metal/semiconductor interfaces) or with the CNL of the other semiconductor determines the direction of charge transfer. At chemisorptive metal/organic semiconductor junctions, the average $(I+A)/2$ has been used[14] to determine the direction of the charge transfer. In light of this, our IDIS-CNL model

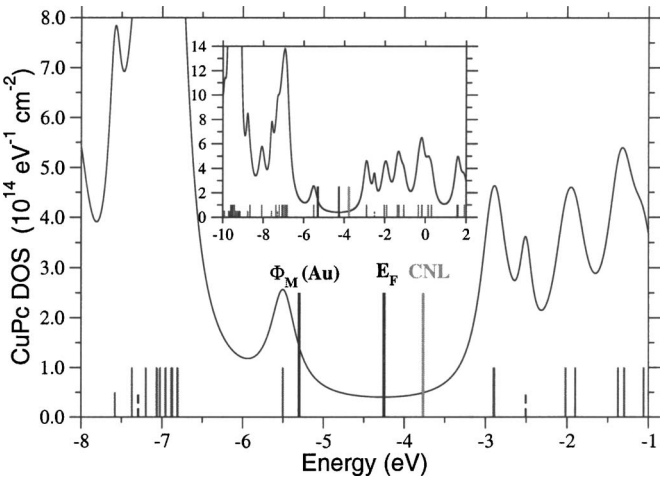

FIG. 3. IDIS, CNL position, metal work function, and interface E_F for the Au/CuPc interface, calculated for d=3.6 Å. Vertical bars represent the CuPc molecular orbitals; in particular, the dashed bars at −7.3 and −2.5 eV correspond to the occupied and empty states strongly localized around the central Cu atom, exhibiting a strong Coulomb repulsion, as discussed in the text.

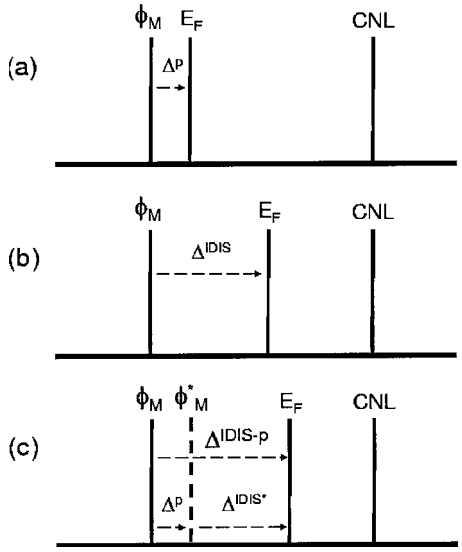

FIG. 4. (a) "Pillow" effect: the reduction of the metal work function due to the orthogonalization of the metal and organic wave functions gives rise to the dipole Δ^p. (b) The IDIS mechanism alone results in the formation of the interface dipole Δ^{IDIS}. (c) Combined IDIS-pillow mechanism: The pillow effect first reduces the metal work function to ϕ^*_M; the offset between ϕ^*_M and the CNL determines the corresponding dipole Δ^{IDIS^*}. The total dipole $\Delta^{IDIS\text{-}p}$ is the sum of both contributions.

can be regarded as an extension to organic materials of the previous proposals. The inclusion of contributions from all molecular levels (not just I and A, which would imply a CNL position always at midgap) yields a CNL position in many cases closer to the lowest unoccupied molecular orbital; experimentally[5] the interface Fermi level is indeed seen to be pinned in the upper part of the gap. This suggests that accurate determination of the CNL position is necessary for the correct description of the molecular level alignment.

We illustrate these ideas for the case of Au/CuPc (Fig. 3): Results for this interface were presented previously[36] but we have recalculated them to include important many-body corrections associated with strongly localized molecular orbitals, as will be described below. In addition, experimental data[38,39] suggest that the metal-CuPc distance d may be larger than what we had originally considered; we have taken the value d=3.6 Å. The integration of the induced DOS yields a CNL position in agreement with previous calculations. Notice that the CNL position is almost unchanged even if d varies, since the empty and occupied states "push" the CNL in opposite directions and cancel each other out. We again find that the position of the CNL within the gap is a robust quantity, very stable against variations of the details of the interaction.

The pinning behavior of the interface is characterized by the screening parameter S_{Au},

$$S_{\mathrm{Au}} = \left[1 + \frac{4\pi e^2 D(E_F) d}{A}\right]^{-1}, \tag{16}$$

where $\mathrm{D}(E_F)$ is the induced DOS (the IDIS) and A is the area associated with each CuPc molecule [$\sim$164 Å^2 (Ref. 31)]. S_{Au} is the slope parameter of the corresponding organic material with Au; these values of S_{Au} are similar, though not exactly equal, to those obtained from a fit to experimental data over a range of different metals.[5] S_{Au} is more dependent on d, which is introduced as an external parameter. Using the calculated values of the CNL and S_{Au} and the experimental work function, we calculate the interface Fermi level position and the induced dipole from [see Fig. 4(b)]

$$E_F - \mathrm{CNL} = S_{\mathrm{Au}}(\phi_M - \mathrm{CNL}), \tag{17}$$

$$\Delta^{\mathrm{IDIS}} = (1 - S_{\mathrm{Au}})(\phi_M - \mathrm{CNL}). \tag{18}$$

For the Au/CuPc, the calculated values CNL=−3.8 eV and S=0.3, and the experimental result of ϕ_M=−5.3 eV (Ref. 38) yields theoretical values for the interface Fermi level, induced dipole, and hole injection barrier of E_F=−4.25 eV, Δ^{IDIS}=1.05 eV, and ϕ_{Bh}=1.25 eV, respectively, to be compared with the experimental results of $E_F^{\mathrm{expt}} = \sim -4.1$, $\Delta^{\mathrm{expt}} = \sim 1.2$, and $\phi_{\mathrm{Bh}}^{\mathrm{expt}}$=1.4 eV, respectively. Notice that the reported experimental value of the ionization potential [i.e., highest occupied molecular orbital (HOMO) position] is −5.5 eV instead of −5.7 eV,[5] that is, 0.2 eV closer to the vacuum than in other works. These values presumably depend on the growth conditions of the organic material[37] and shift the molecular electronic spectrum. In order to make a direct comparison with these experimental results, therefore, we too have shifted the organic electronic spectrum by 0.2 eV, resulting in a shift of the CNL position from −4.0 (Ref. 36) to −3.8 eV.

Importantly, the CuPc molecule has an odd number of electrons, and a singly occupied molecular orbital is obtained as the HOMO of the DFT calculation. This molecular state is strongly localized around the central Cu atom. DFT is known to greatly underestimate molecular gaps, and the problem of molecular level positions is even more acute for the case of this state, where Coulomb repulsion plays an important role which DFT is unable to describe properly. When the position of the molecular levels, and, in particular, this Cu-related state, is appropriately corrected for,[21] we obtain the positions shown in Fig. 3 (dashed vertical bars at −7.3 and −2.5 eV). In particular, the correct position of this strongly localized

state is shifted deeper in the spectrum with respect to the DFT calculation, while the empty state associated with it is closely related to the Coulomb repulsion, yielding $U^{\text{eff}}=4.8$ eV at the interface (compared to 7.0 eV for the isolated molecule) for this molecular state.[40] A correction of DFT molecular levels is needed for the correct description of the energy level alignment and the CNL position, not only in cases where many-body effects play an important role (as in the case of this Cu-localized molecular orbital), but in general for cases where charge excitations are localized, as is the case of most organic semiconductors: the "Koopmans shifts"[21] act on each molecular orbital shifting it accordingly, so that the result is not a rigid shift of the occupied and empty parts of the spectrum but introduce some shuffling of the molecular levels. They increase the molecular gap with respect to the DFT results and, together with a correction of the gap at the interface due to electronic polarization,[41] are necessary for a correct analysis of the energy level alignment.

V. UNIFIED PILLOW INDUCED DENSITY OF INTERFACE STATES MODEL

The two mechanisms outlined above can be simultaneously described within the unified model we now describe (see Fig. 4).

(i) Consider first how ϕ_M is modified due to the pillow effect [Fig. 4(a)]. The overlap between the metal and molecular wave functions gives rise to the contribution Δ^p, which reduces the metal work function (i.e., makes it less negative). This amounts to changing ϕ_M to the effective work function $\phi_M^*=\phi_M-\Delta^p$ (where Δ^p is negative).

(ii) In a second step, the interface relaxes by transferring charge between the metal and the organic molecule [Fig. 4(b)]. Using the IDIS formalism, this dipole is [see Eq. (8)] $\Delta^{\text{IDIS}^*}=(1-S)(\phi_M^*-\text{CNL})=(1-S)(\phi_M-\Delta^p-\text{CNL})$.

(iii) The total dipole at the interface is the sum of both contributions [shown consecutively in Fig. 4(c)],

$$\Delta^{\text{IDIS-}p}=\Delta^p+\Delta^{\text{IDIS}^*}=\Delta^p+(1-S)(\phi_M-\Delta^p-\text{CNL})$$
$$=(1-S)(\phi_M-\text{CNL})+S\Delta^p. \quad (19)$$

Equation (19) shows how Δ interpolates between the two limits: When $S=1$, there is no screening at the interface and $\Delta=\Delta^p$; all the dipole comes from the pillow effect and this controls the Fermi level position. When $S=0$, on the other hand, $\Delta=\phi_M-\text{CNL}$ and $E_F=\text{CNL}$: The Fermi level is completely pinned at the CNL, and the pillow effect does not play a role since it is fully screened. Notice how, in our combined formalism, the pillow effect is first considered and then the IDIS acts on the remaining potential difference (i.e., $\phi_M^*-\text{CNL}$); equivalently, this amounts to the usual IDIS mechanism plus the screened pillow contribution ($S\Delta^p$). Thus, as shown by the last term of Eq. (19), the pillow effect is present at the interface but its effect is reduced by the corresponding screening parameter, as will be seen in the results.

TABLE I. Calculated values of the CNL position, S parameter, and "pillow" dipole, as well as experimental values of the Au work function (Refs. 4, 7, 9, and 38) for the interfaces between Au and the organic materials considered.

	PTCDA	PTCBI	CBP	CuPc
CNL (eV)	−4.8	−4.4	−4.05	−3.8
ϕ_M^{exp} (Au) (eV)	−5.1	−5.0	−4.9	−5.3
S	0.16	0.16	0.50	0.30
Δ^p (eV)	0.89	1.09	0.42	0.73

VI. RESULTS AND DISCUSSION

Table I presents our results for the CNL position, S parameter, and pillow dipole Δ^p for interfaces between Au and PTCDA, PTCBI, CBP, and CuPc, as well as the experimental metal work function measured in each case. The values of Δ^p can be intuitively understood in terms of geometrical factors of the molecules: Δ^p is larger the more closely packed the benzene rings are and the smaller the metal-organic distance is, since orthogonalization effects will be stronger.

In order to compare the pillow and the IDIS models, we calculate the three interface dipoles (pillow, IDIS, and unified IDIS-pillow) and compare them in Table II, where the value of ϕ_M is taken from experiment in each case. The values of S_{Au}, CNL, and Δ^p are theoretical inputs, while ϕ_M is the experimental measurement for each case. Since ϕ_M presumably depends on the growth conditions,[42] we think it is more appropriate to use the measured (which reflects the experimental conditions of each particular case), rather than a calculated, work function in order to perform a more direct comparison with experiment. As for the CNL positions, they ultimately depend on the ionization and affinity levels; if the experimental conditions change these values significantly, then the whole gap is shifted and the CNL should be shifted accordingly, as was mentioned in the Au/CuPc case for the ionization level. This shows how theory and experiment are combined in the study of these junctions, as the knowledge of S_{Au}, CNL, Δ^p, and ϕ_M enable the prediction of interface properties.

The data of Table II show a good agreement with experiment, with Au/PTCDA and Au/PTCBI slightly overestimating the experimental values (experimental values are referred to molecular level centers, rather than edges, by adding 0.5 eV). Notice from this table that the dipoles and injection

TABLE II. Interface dipoles and injection barriers with Au resulting from the pillow [Eq. (13)], IDIS [Eq. (18)], and combined IDIS-pillow [Eq. (19)] models, as well as experimental (Refs. 4, 7, 9, and 38) results.

	PTCDA	PTCBI	CBP	CuPc
Δ^p (eV)	0.89	1.09	0.42	0.73
Δ^{IDIS} (eV)	0.25	0.50	0.43	1.05
$\Delta^{\text{IDIS-}p}$ (eV)	0.39	0.67	0.64	1.27
Δ^{exp} (eV)	~0.25	0.4	0.5	~1.2
ϕ_{Bh}^p (eV)	3.09	2.79	2.32	1.13
$\phi_{\text{Bh}}^{\text{IDIS}}$ (eV)	2.45	2.20	2.33	1.25
$\phi_{\text{Bh}}^{\text{IDIS-}p}$ (eV)	2.59	2.37	2.54	1.47
$\phi_{\text{Bh}}^{\text{exp}}$ (ev)	2.4	2.1	2.4	1.4

barriers coming only from the pillow effect can differ from the experimental value by almost as much as 0.5 eV. This shows that this mechanism alone cannot explain the observed properties. In addition, notice that the values calculated using the IDIS and IDIS-pillow models are quite similar, with differences of 0.1–0.2 eV. Given the experimental resolution of ~0.1 eV,[5] this explains why the IDIS model (without considering the pillow effect) has been so successful: The inclusion of the pillow is a correction to the IDIS results but does not modify it significantly. This shows that the contribution coming from the pillow effect should be included, but the IDIS model already represents a good description of the energy level alignment.

VII. DISCUSSION AND CONCLUSIONS

We have presented a unified model which presents a combined description of the "pillow" and IDIS effects at metal/organic interfaces. Our results show that, for the interfaces considered, the pillow effect can modify the values of the IDIS model, but that these modifications are generally small and that the IDIS model alone represents a good approximation to the energy level alignment problem.

As commented above, this is related to the screening at the interface: When screening is strong, the Fermi level will be pinned near the CNL; simultaneously, the pillow effect will too be screened [see the last term of Eq. (19)]. On the other hand, weakly screening interfaces will be characterized by a Fermi level which can move more freely within the gap. This means that the pillow contribution (which in turn will be larger since it is less screened) will be more significant.

We thus expect the pillow effect to be more significant in those interfaces where screening is weak; this can result, for example, from a large metal-organic distance d. We believe this situation to be appropriate for the case of benzene/Cu(111), which was recently analyzed theoretically by Bagus *et al.*[30] The authors reported a contribution of $0.92D$ (or $0.153D$ per C atom) to the induced interface dipole coming from the orthogonalization of the molecular and metal wave functions, as well as from geometrical molecular deformations. From our results for the interfaces considered, we obtain a dipole per C atom ranging $(0.08–0.14)D$. Since many factors will probably be different in both interfaces, our intention here is not to make a quantitative evaluation but to state that our results are comparable to the more sophisticated CSOV calculations of Bagus *et al.* and thus provide an appropriate description of this effect.

To summarize, we have presented a unified model which combines the description of two major mechanisms taking place at metal/organic interfaces: The compression of the metal electronic tail due to the orthogonalization with the adsorbed molecules (the pillow effect) and the induced DOS. We find that the pillow effect introduces some corrections to the IDIS model, but they do not alter the main physical results, which can be well approximated by the induced DOS model only. While the pillow effect is not important at organic heterojunctions due to the weak interaction between the two organic materials (as demonstrated experimentally using a polymer electrode[43]), it is nevertheless important at metal/organic interfaces: The pillow and IDIS effects are intrinsic to these interfaces and will be present at every metal/organic junction. Therefore, we believe that a combined, unified description of both mechanisms is important and will contribute to the understanding of the energy level alignment at these interfaces.

ACKNOWLEDGMENTS

The authors gratefully acknowledge financial support by the Universidad Autónoma de Madrid, the Juan de la Cierva program, the Spanish CICYT under Project Nos. MAT 2001-0665, MAT 2004-01271, and NAN-2004-09183-C10-07 and the Comunidad de Madrid/FEDER under Project No. 07N/0050/2001.

[1] S. R. Forrest, Nature (London) **428**, 911 (2006).
[2] J. Campbell Scott, J. Vac. Sci. Technol. A **21**, 521 (2003).
[3] S. Narioka, H. Ishii, D. Yoshimura, M. Sei, Y. Ouchi, K. Seki, S. Hasegawa, T. Miyazaki, Y. Harima, and K. Yamashita, Appl. Phys. Lett. **67**, 1899 (1995).
[4] I. G. Hill, A. Rajagopal, A. Kahn, and Y. Hu, Appl. Phys. Lett. **73**, 662 (1998).
[5] C. Shen, A. Kahn, and I. G. Hill, in *Conjugated Polymer and Molecular Interfaces*, edited by W. R. Salaneck, K. Seki, A. Kahn, and J. J. Pireaux (Marcel Dekker, New York, 2001), pp. 351–400.
[6] H. Ishii, K. Sugiyama, E. Ito, and K. Seki, Adv. Mater. (Weinheim, Ger.) **11**, 605 (1999).
[7] I. G. Hill, J. Schwartz, and A. Kahn, Org. Electron. **1**, 5 (2000).
[8] C. Shen and A. Kahn, Org. Electron. **2**, 89 (2001).
[9] I. G. Hill, A. Rajagopal, and A. Kahn, J. Appl. Phys. **84**, 3236 (1998).
[10] M. Eremtchenko, D. Bauer, J. A. Schaefer, and F. S. Tautz, New J. Phys. **6**, 4 (2004).
[11] S. Kera, Y. Yabuuchi, H. Yamane, H. Setoyama, K. K. Okudaira, A. Kahn, and N. Ueno, Phys. Rev. B **70**, 085304 (2004).
[12] M. Knupfer and G. Paasch, J. Vac. Sci. Technol. A **23**, 1072 (2005).
[13] P. S. Bagus, V. Staemmler, and C. Wöll, Phys. Rev. Lett. **89**, 096104 (2002).
[14] X. Crispin, V. Geskin, A. Crispin, J. Cornil, R. Lazzaroni, W. R. Salaneck, and J. L. Brédas, J. Am. Chem. Soc. **124**, 8131 (2002).
[15] X. Crispin, Sol. Energy Mater. Sol. Cells **83**, 147 (2004).
[16] H. Vázquez, R. Oszwaldowski, P. Pou, J. Ortega, R. Pérez, F. Flores, and A. Kahn, Europhys. Lett. **65**, 802 (2004).
[17] H. Vázquez, F. Flores, R. Oszwaldowski, J. Ortega, R. Pérez, and A. Kahn, Appl. Surf. Sci. **234**, 108 (2004).
[18] H. Vázquez, F. Flores, and A. Kahn, Org. Electron. **8**, 241 (2007).
[19] Y. J. Dappe, R. Oszwaldowski, P. Pou, J. Ortega, R. Pérez, and F. Flores, Phys. Rev. B **73**, 235124 (2006).
[20] P. Pou, R. Oszwaldowski, H. Vázquez, R. Pérez, F. Flores, and J. Ortega, Int. J. Quantum Chem. **91**, 151 (2002).
[21] R. Oszwaldowski, H. Vázquez, P. Pou, J. Ortega, R. Pérez, and F. Flores, J. Phys.: Condens. Matter **15**, S2665 (2003).
[22] M. V. Basilevsky and M. M. Berenfeld, Int. J. Quantum Chem. **6**, 23 (1972).
[23] V. Kvaniska, V. Laurinc, and I. Hubac, Phys. Rev. A **10**, 2016 (1974).
[24] I. C. Hayes and A. J. Stone, Mol. Phys. **53**, 83 (1984).
[25] P. R. Surjan, C. Pérez del Valle, and L. Lain, Int. J. Quantum Chem. **64**, 43 (1997).
[26] V. Lukes, V. Laurinc, and S. Biskupic, Int. J. Quantum Chem. **75**, 81 (1999).
[27] B. Jeziorski and W. Kolos, Int. J. Quantum Chem. **12**, 91 (1977).
[28] S. Rybakm, B. Jeziorski, and K. Szalewicz, J. Chem. Phys. **95**, 6576 (1991).
[29] K. Patkowski, B. Jeziorski, and K. Szalewicz, J. Chem. Phys. **120**, 6849 (2004).
[30] P. S. Bagus, K. Hermann, and C. Wöll, J. Chem. Phys. **123**, 184109 (2005).
[31] T. S. Ellis, K. T. Parka, S. L. Hulbert, M. D. Ulrich, and J. E. Rowe, J. Appl. Phys. **95**, 982 (2004).
[32] P. Fenter, P. E. Burrows, P. Eisenberger, and S. R. Forrest, J. Cryst. Growth **152**, 65 (1995).

[33] T. Schmitz-Hübsch, T. Fritz, F. Sellam, R. Staub, and K. Leo, Phys. Rev. B **55**, 7972 (1997).
[34] P. Fenter, F. Schreiber, L. Zhou, P. Eisenberger, and S. R. Forrest, Phys. Rev. B **56**, 3046 (1997).
[35] C. Tejedor, F. Flores, and E. Louis, J. Phys. C **10**, 2163 (1977).
[36] H. Vázquez, W. Gao, F. Flores, and A. Kahn, Phys. Rev. B **71**, 041306(R) (2005).
[37] S. M. Tadayyon, H. M. Grandin, K. Griffiths, L. L. Coatsworth, P. R. Norton, H. Aziz, and Z. D. Popovic, Org. Electron. **5**, 199 (2004).
[38] H. Peisert, M. Knupfer, T. Schwieger, J. M. Auerhammer, M. S. Golden, and J. Fink, J. Appl. Phys. **91**, 4872 (2002).
[39] M. Knupfer (private communication).
[40] H. Vázquez, Ph.D. thesis, Universidad Autónoma de Madrid, Madrid, Spain, 2006.
[41] E. V. Tsiper, Z. G. Soos, W. Gao, and A. Kahn, Chem. Phys. Lett. **360**, 47 (2002).
[42] A. Wan, J. Hwang, F. Amy, and A. Kahn, Org. Electron. **6**, 47 (2005).
[43] N. Koch, A. Kahn, J. Ghijsen, J.-J. Pireaux, J. Schwartz, R. L. Johnson, and A. Elschner, Appl. Phys. Lett. **82**, 70 (2003).